Studies on Spread Monolayers and LB Films of Long-Chain Alkylchlorosilanes by Brewster Angle Microscopy and X-Ray Photoelectron Spectroscopy

Ken-ichi Iimura, Noboru Suzuki, and Teiji Kato*

Department of Applied Chemistry, Faculty of Engineering, Utsunomiya University, Utsunomiya 321

(Received October 4, 1995)

Long-chain alkylchlorosilanes (trichloro(octadecyl)silane; TCOS, dichloro(methyl)(octadecyl)silane; DCMOS, and chloro(dimethyl)(octadecyl)silane; CDMOS) form stable spread monolayers on water surfaces. From the experimental fact that X-ray photoelectron spectra of the LB films showed no chlorine peak, it is estimated that chlorosilyl residues were hydrolyzed rapidly just after spreading on the water surface. Brewster angle microscopic observation of the monolayers gave information on the molecular tilt and phase transitions in these monolayers with compression. It is expected that dimerization or polymerizations of resultant hydroxysilane residues could proceed by condensation among the hydroxyl groups in monolayers. However, condensation reactions were very slow in neutral conditions and the film molecules exist mainly as monomeric or dimeric hydroxysilanes and not in polymeric forms, based on the comparison of the atomic ratios of Si to O estimated from the X-ray photoelectron spectroscopy measurements of LB films of the three compounds and those of the polymers of TCOS and DCMOS, and the dimer of CDMOS.

There is a growing interest in both Langmuir–Blodgett (LB), and self-assembled (SA) films as ordered ultrathin organic materials.[1] Long-chain alkylchlorosilanes and methoxy- or ethoxyalkylsilanes are representative materials of SA films for modifying polar solid surfaces, having OH groups such as many metal oxides that become hydrophobic upon treating the solids in dehydrated organic solutions of them. There are many papers reporting structures and properties of SA monolayers on solid surfaces.[2—6] Sagiv and his associates have developed a constructive technique for making layered structures using SA monolayers of modified long-chain alkylsilanes on solid surfaces.[7,8] Ulman has reviewed SA monolayers of alkyltrichlorosilanes.[9]

There are some papers dealing with studies on the structure and properties of spread monolayers of long-chain trichloro- or triethoxyalkylsilanes at the water surface. Okahata and Ariga have studied π–A isotherms of polymerized monolayers of single-, double-, and triple-chain ethoxyalkylsilanes at the water surface.[10,11] Sjöblom and his co-workers have discussed the mechanism of hydrolysis and condensation of trimethoxyalkylsilanes in monolayers.[12] Barton and his co-workers have written a short paper dealing with a glazing angle X-ray diffraction study on polymerized trichloro(octadecyl)silane monolayers at the water surface.[13] Daillant and his research group have discussed buckling of polymerized trichloro(octadecyl)silane monolayers by measuring grazing incidence synchrotron X-ray diffraction.[14]

However, details of hydrolysis and condensation reactions in monolayers of alkylchlorosilanes still remain rather ambiguous. Moreover, there is no paper dealing with a study on the structure and properties of spread monolayers of di-chloro- and monochloro-long-chain alkylsilanes.

This paper reports properties and structures of spread monolayers of trichloro(octadecyl)silane, dichloro(methyl)-(octadecyl)silane, and chloro(dimethyl)(octadecyl)silane at a distilled water surface, based on the π–A isotherms and BAM observation of monolayers, and discusses hydrolysis and condensation in monolayers using the pH dependency of isotherms and X-ray photoelectron spectroscopy (XPS) measurements of the LB films.

Experimental

Trichloro(octadecyl)silane (> 98%, abbreviated hereafter as TCOS) was purchased from Merck Chemicals. Dichloro(methyl)-(octadecyl)silane (> 97%, DCMOS) was purchased from Chisso Co., Ltd., Chloro(dimethyl)(octadecyl)silane (> 96%, CDMOS) was purchased from Tokyo Kasei Chemicals. Purity of materials was checked by 220 MHz NMR in solutions of deuterated chloroform. They were used as film materials without further purification. Spreading solutions were prepared with spectrograde hexane (Dojin Chemicals) of concentration around 2.5×10^{-6} mol ml^{-1}. Freshly distilled water with an all Pyrex®-made distilling apparatus was used as the subphase.

A microcomputer-controlled instrument for measuring π–A isotherms of monolayers was constructed in our laboratory. The most important feature of this instrument is that two barriers confining monolayers are driven symmetrically in all compression modes, including constant strain rate compression. A precisely temperature-programmable very shallow Langmuir trough (inside dimensions, 40L×17D×0.2D cm^3) was developed using a large number of integrated Peltier element modules. Surface temperature of the subphase water can be precisely controlled according to control programs including isothermal, linear heating, linear cooling, and combinations of these modes. Surface temperature of the water

in the trough is detected by a platinum wire resistance temperature sensor of very small heat capacity, sealed in a piece of nickel-plated copper, and is taken into the microcomputer via an A/D converter. In isothermal control, fluctuation of the surface temperature was very small (±0.009 °C at 10 °C and ±0.007 °C at 20 °C). Surface pressure was detected with a modified Wilhelmy type surface balance. Sensitivity of the surface balance was higher than 0.01 mN m^{-1}. Details of the newly developed trough have been reported elsewhere.[15] All isotherms were measured at 20 °C throughout this work unless otherwise described.

Monolayers were spread on the water surface with a gas-tight type microsyringe. Compression of the monolayers started 30 min after spreading to assure complete evaporation of the spreading solvent.

A Brewster angle microscope (BAM) was also constructed in our laboratory. It is composed of a 10 mW He–Ne laser, a Gran–Thompson polarizer, a quarter wave plate, an analyzer, a zooming microscope of long working distance (Seiwa Optical Industry Co., Ltd., MS-501), and a CCD camera of very high sensitivity (Flobel Optics Co., Ltd., HCC-600M, 0.01 lux at the highest sensitivity). BAM images are taken into a videorecorder and printed out with a color videoprinter.

XPS spectra of LB samples were recorded on an ESCA 5600 (Perkin Elmer) spectrometer using a monochromatic Al $K\alpha$ source run at 14 kV, 300 W and at a take-off angle of 85°. The shape of the spectra indicated that no correction for surface charging was needed except for polymer samples where a neutralizer (an electron gun for compensating induced positive charge of samples due to the photoionization by the X-ray) was used to eliminate the effect of charging. The binding energy scale was calibrated to set the main C1s (C–C) feature at 284.6 eV. Spectra were run in both low resolution (pass energy 188 eV) and high resolution (pass energy 59 eV) modes for O1s, Si2s, and Si2p regions. Elemental ratios were calculated from the satellite-subtracted high resolution spectra normalized for constant transmission using a newly developed layered structure model, which is reported elsewhere.[16] The sensitivity factors used in the computations were O1s = 39.90, Si2s = 17.91, and Si2p = 15.73, respectively, according to the manual of the instrument.

The monolayers were transferred onto glass slides of the optical microscope by the conventional vertical dipping method. The glass substrates were covered with vacuum-deposited gold of about 1 μm thickness to discriminate XPS peaks of Si and O in LB films from those of the glass substrate. DCMOS and CDMOS monolayers were deposited in Y-type but TCOS monolayers were transferred by X-type deposition. However, X-ray diffraction measurements of LB films revealed that all were Y-type structures. This means that TCOS monolayers do overturn during deposition with the vertical dipping method.[17] Polymer and dimer samples were set on gold-covered glass plates and melted by heat in a vacuum to adhere to the substrates.

Results and Discussion

Surface pressure(π)–molecular area(A) isotherms give much information on the properties of monolayers at the water surface. We have proposed a concept of the time of observation of π–A measurements of monolayers at the water surface.[18] The time of observation is defined as the reciprocal of the strain rate of compression of the monolayers. When film materials form rather condensed monolayers under experimental conditions, the shape of the isotherms is mainly governed by the balance between the relaxation times of the molecular processes that occur in the monolayers during compression and the time of observation.

Figure 1 shows π–A isotherms of TCOS monolayers on the distilled water surface, measured under two times of observation (t_{ob} = 600 and 6000 s). TCOS forms condensed monolayers and the minimum compressibility of the condensed region is as small as 0.0029 m mN^{-1}. At an observation time increased by a factor of 10, collapse pressure drops only by several mN m^{-1}. This means that the monolayer is tolerably stable. The limiting molecular area is 0.205 nm^2/molecule, corresponding to a cross section area of an alkyl chain. These features of the monolayer suggest that TCOS molecules are not in polymeric form because pectinated polymer amphiphile monolayers occupy larger molecular areas than those of corresponding monomeric monolayers in general, due to the conformational and/or configurational restriction of main chains at the water surface.

Figure 2 shows BAM images of a TCOS monolayer during isotherm measurements at the observation time of 600 s. The points of BAM observation are marked on the isotherm in Fig. 1. The image (A) shows that there are irregular macroscopic and sharp-edged domains of lateral size of a few mm in the spread monolayer of TCOS even before starting compression. This means that the interactions among TCOS molecules are rather strong and the molecules gather to form the domains spontaneously without compression. These macroscopic domains are gathered by compression and are fused with the lateral pressure. At point (B) the surface pressure starts to rise, BAM image (B) shows there still remain some open spaces among the fused macroscopic domains. BAM image (C) shows that the open space becomes

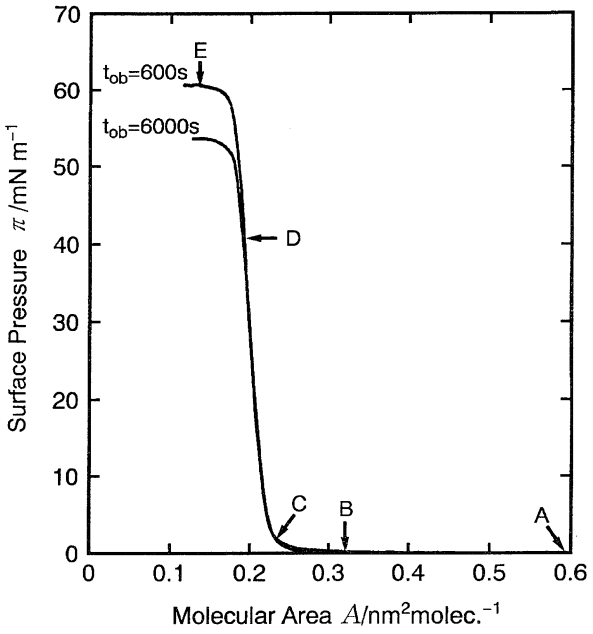

Fig. 1. π–A isotherms of spread monolayers of TCOS at the distilled water surface at two times of observation (600 and 6000 s). Points of BAM observation during compression are marked on the isotherm of t_{ob} = 600 s.

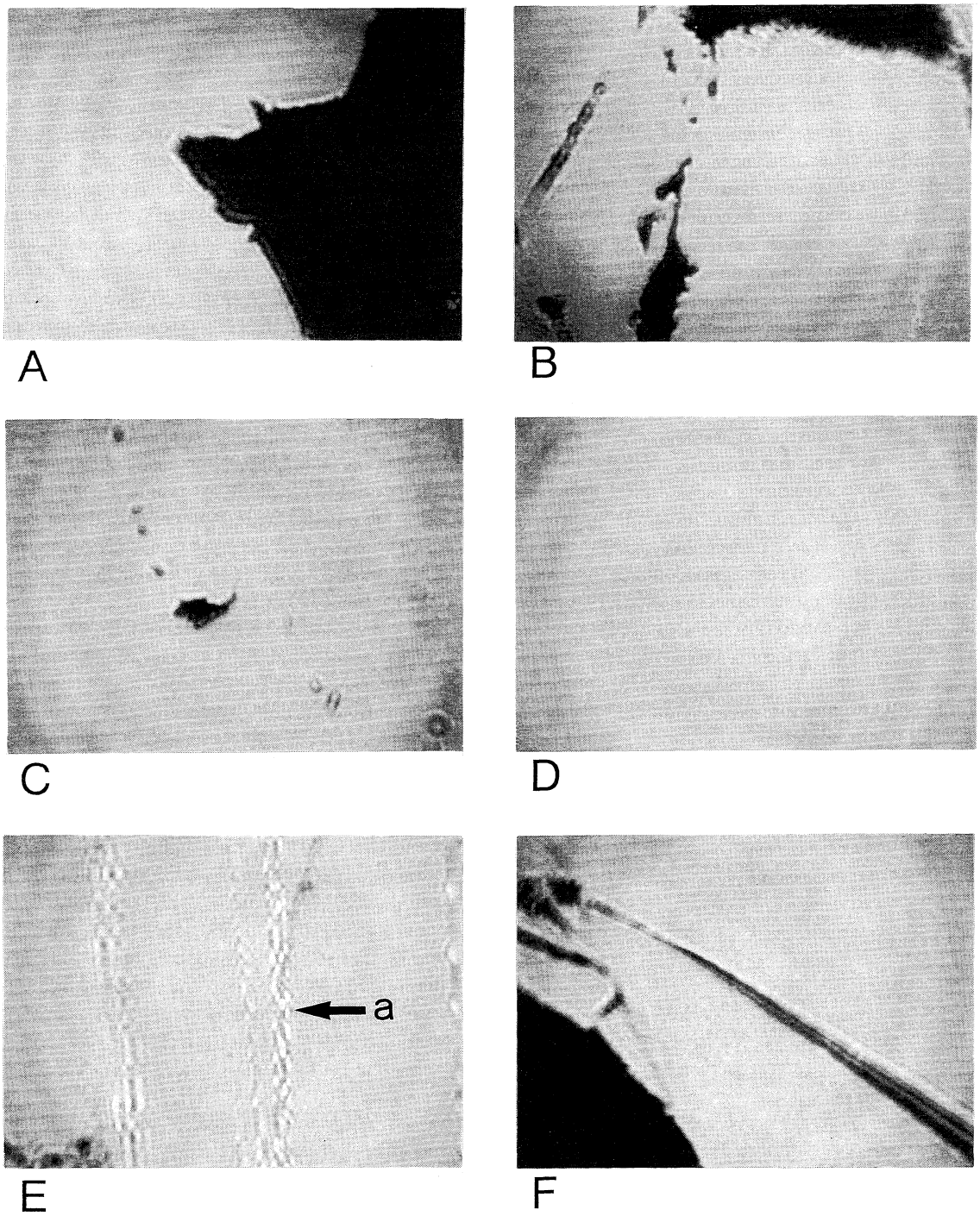

Fig. 2. BAM images of a spread monolayers of the TCOS monolayer observed during measurement of the isotherm in Fig. 1. The scale bar in (A) represents 300 μm. (See text for details.)

small with external compression and the monolayer looks almost uniform at a surface pressure above 10 $mN\,m^{-1}$ as shown in the image (D). At the surface pressure above 55 $mN\,m^{-1}$, the monolayer starts to collapse with compression and the image shows some stripes or ridges of the collapsed structure (arrow a) as shown in the image (E). When the monolayer is expanded suddenly just before the collapse point, the surface pressure drops rapidly to almost zero and brittle breaks of the film results in sharp-edged fragments of the film, as shown in the image (F).

BAM images indicate a molecular tilt in the monolayers by rotating an analyzer in the detecting optical path. When all alkyl chains in monolayers stand normal to the water surface or they are in the liquid state, we cannot observe optical anisotropy in monolayers with BAM. TCOS monolayers reflect laser light rather strongly and do not have optical anisotropy throughout the measurement of isotherms.

It has been reported that the vibrational frequencies of the CH_2 antisymmetric and symmetric stretching bands are very sensitive to the structure of the hydrocarbon chain.[19]

Spectra are not shown here but FT-IR measurements of the LB films of TCOS on CaF_2 plates (transmission absorption spectra) and on fused quartz plates (external reflection absorption spectra) show that the bands always appear near 2918 and 2949 cm^{-1}, not dependent on the molecular area. These wave numbers of absorption suggest that alkyl chains are all in the trans-zigzag conformation even in the isolated macroscopic domains before starting compression. These experimental facts of BAM and FT-IR measurements indicate that alkyl chains in TCOS monolayers should always stand normal to the water surface.

Figure 3 shows π–A isotherms of DCMOS monolayers measured under two t_{ob} of 600 s and 6000 s. DCMOS also forms rather condensed monolayers but the minimum compressibility of the condensed region, 0.0056 m mN^{-1}, is much larger than that of the TCOS monolayers. The onset molecular area of the pressure rise on the isotherms is also larger than that of TCOS, possibly due to the methyl group in the hydrophilic moiety. The limiting molecular area (0.33 nm^2/molec.) is also much larger than that of simple-chain amphiphiles such as long-chain acids or alcohols. These facts suggested that the large limiting molecular area of DCMOS monolayers may be determined by the cross-sectional area of the hydrophilic group of the DCMOS molecule. After collapse, surface pressure drops rather quickly, in contrast to TCOS, but the collapse pressure itself is not changed much by the change of t_{ob} for ten times longer.

Figure 4 shows BAM images of a DCMOS monolayer during measurement of the isotherm at t_{ob} of 600 s. The points of BAM observation are marked on the isotherm in Fig. 3. Image (A) shows a macroscopic domain, before starting compression of the monolayer. The shape of the domain

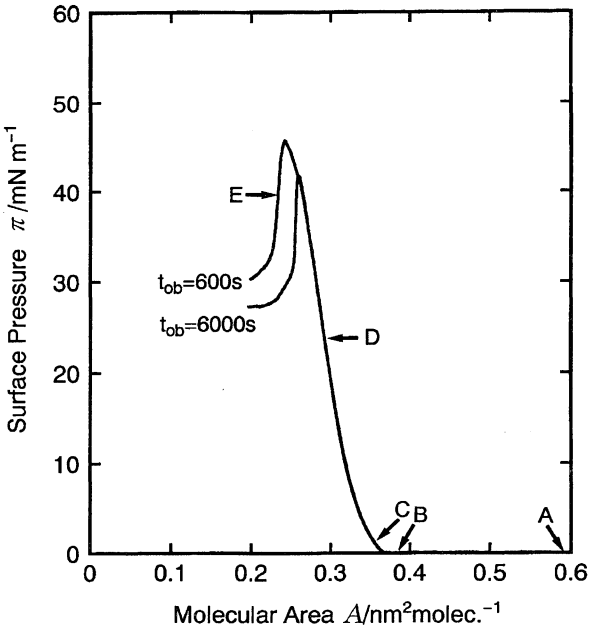

Fig. 3. π–A isotherms of spread monolayers of DCMOS at the distilled water surface at two times of observation (600 and 6000 s). Points of BAM observation during compression are marked on the isotherm of t_{ob} = 600 s.

is not as angular as TCOS, but, rather smoothly curved. We can see a fringe structure of the domain in contrast to the sharp edges of domains of TCOS. Macroscopic domains gather by compression and fuse. Fusion of the domains is easier than in the case of TCOS monolayers because of the fluid character of the DCMOS monolayers. At point (B) just before the onset of pressure rise, some open spaces where molecular density may be low are still observed among the fused domains. At the lower surface pressure around point (C), we can see low molecular density regions in the film as shown in the image (C) (arrow a). These low density regions disappear at around 10 mN m^{-1} with compression and the monolayer becomes uniform above this pressure as the image (D) shows. At a surface pressure above 35 mN m^{-1}, granular-type collapsed structure starts to appear and the number and the size of the collapsed structures increases with compression. We can observe numerous collapsed granules in the image (E) after the collapse point. When barriers are manipulated to expand the monolayer with the same strain rate at just before the collapse point, the isotherm closely follows that of compression and a low density region appears again as seen in image (F) (arrow b).

Figure 5 shows π–A isotherms of CDMOS monolayers at the water surface under the two t_{ob} of 600 and 6000 s and a surface compressibility ($\varkappa^S$)-molecular area (A) relation calculated from the numerical differentiation of the isotherm of 600 s. CDMOS monolayers have expanded-type complex isotherms and they show some phase transitions with compression; the $\varkappa_S$–A relation shows two minima in the liquid-expanded region (M_1 and M_2) and after the minima there are two maxima corresponding to the two plateaux on the isotherm. The minimum compressibility is as small as 0.0039 m mN^{-1} at around 0.20 nm^2/molec. It is interesting to note here that the so-called solid film region (the steepest region of the isotherm) disappears under the measurement of the longer t_{ob} of 6000 s. This means that the relaxation times of the molecular processes of the partial collapse in the solid film region that lower the surface pressure are shorter than the time of observation, 6000 s under these experimental conditions.

Figure 6 shows BAM images of a CDMOS monolayer during measurement of the isotherms at t_{ob} of 600 s. The points of BAM observation are marked on the isotherm in Fig. 5. At the point (A), small numbers of circular domains started to appear even before the start of the phase transition at point (B). From the point (B) to point (D) (through (C)) the number and the size of the circular domains increase with compression as shown in images (B) to (D). Before completion of the first step of phase transition, the second kind of domains starts to appear at point (E) as seen from the image (E). The second phase transition proceeds from point (F) to (H) and the first phase transition is nearly completed at point (F). Thus, the two phase transitions partly overlap each other. The second phase transition is not completed even at point (I) as seen from the image (I). The monolayer becomes uniform near the point (J). Formation of the three-dimensional structures by the partial collapse has already

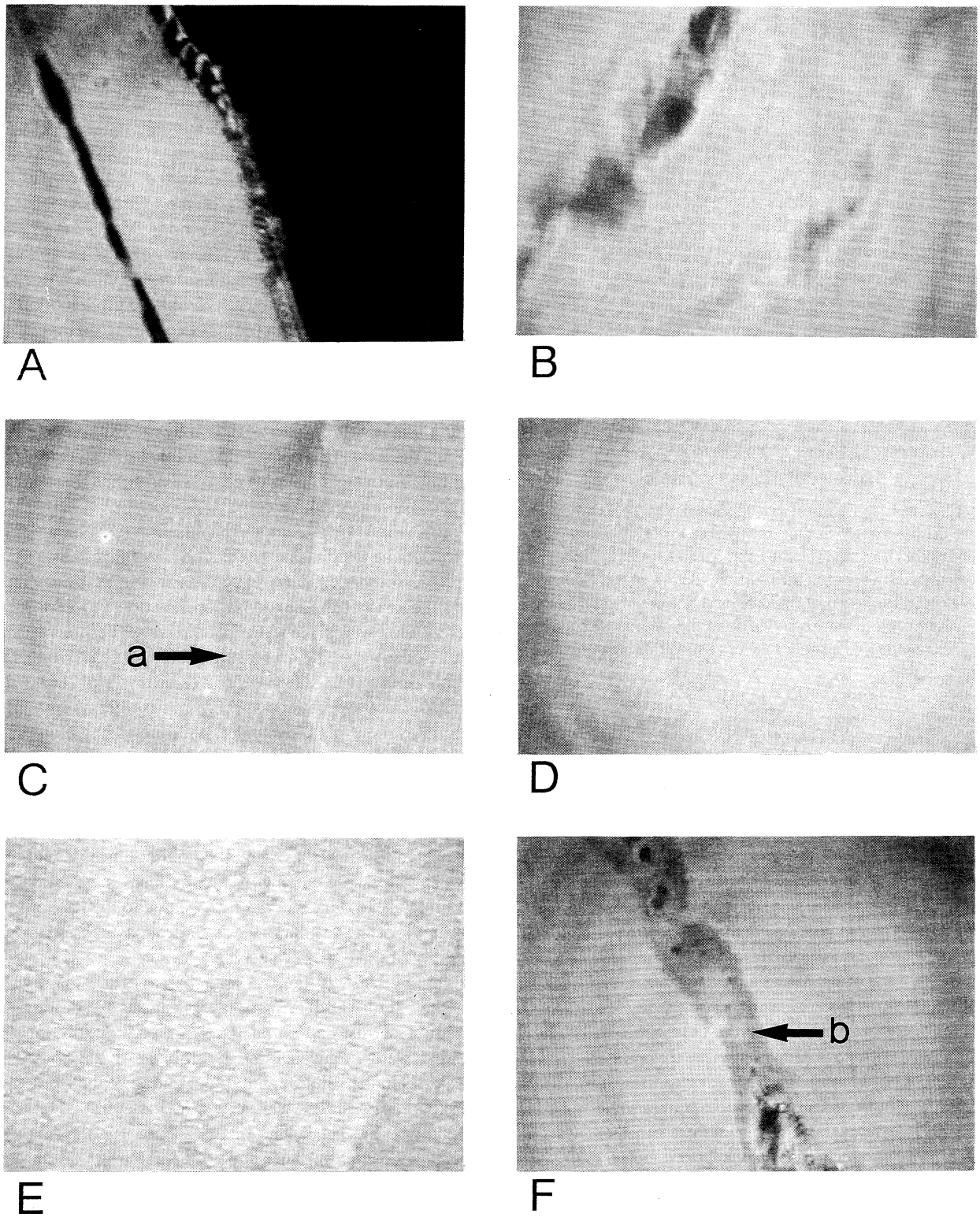

Fig. 4. BAM images of the spread monolayer of DCMOS during measurement of the isotherm in Fig. 3. The magnification of photo is same as to that in Fig. 2. (See text for details.)

started in what is called the solid film region as shown in the image (K). These collapsed granules grow further with compression as seen in the image (L).

Figure 7 shows the XPS of LB films of TCOS (A) and TCOS polymer (B) on the gold-covered glass plate. The procedure to obtain a TCOS polymer will be described later. Five monolayers were transferred onto the substrate to make clear peaks of the elements of LB films by weakening or concealing the peaks of Au. However, weak peaks of Au were observed for the LB sample at 335.1 eV ($Au4d_{5/2}$) and 352.7 eV ($Au4d_{3/2}$), possibly due to the higher sensitivity of Au4d electrons (six times higher than that of Si2s electrons),

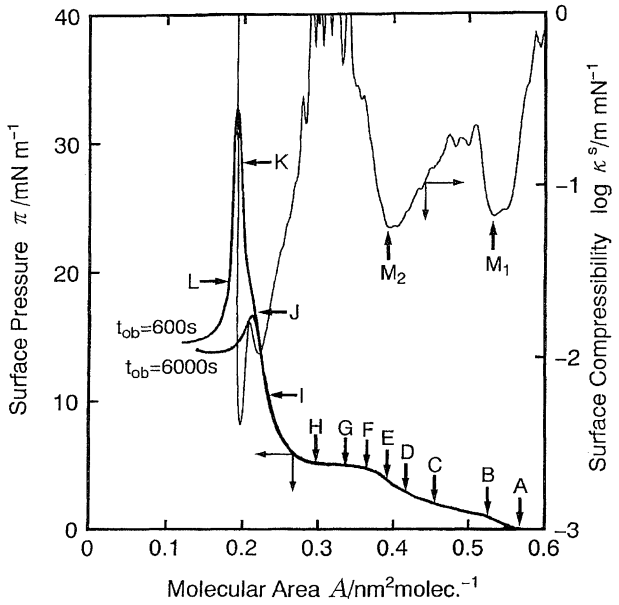

Fig. 5. π–A isotherms of spread monolayers of CDMOS at the distilled water surface at two times of observation (600 and 6000 s), and the surface compressibility (κ^s)–A relation calculated by the numerical differentiation of the isotherm of t_{ob} = 600 s. Points of BAM observation are marked on the isotherm. Note that so-called solid film region disappears on the isotherm of longer time of observation. (See text for details.)

thinness of the LB film, and rather quick desorption of the TCOS LB films in the ultrahigh vacuum of the XRS chamber (2×10^{-8} Pa); escape depth of Au4d electrons of about 3 nm and the thickness of the 5-layer LB film of TCOS, 12.5 nm give a possible escape of Au4d electrons as 1.5%. In fact, about 20% peak reduction of TCOS LB films was observed for 300 min in vacuum, in contrast, no peak reduction was observed for the TCOS polymer film. This is one evidence of the monomeric character of the TCOS molecules in the monolayer under neutral conditions. XPS of the TCOS polymer film gives no Au4d peak because of the sample thickness as shown in Fig. 7(B).

If chlorine atoms are included in the LB films, we should detect a peak around 199 eV (chlorine $2p_{3/2}$ peak).[20] However, there was no peak corresponding to the strongest peak of chlorine in both spectra even under higher sensitivity measurements. Spectra are not shown here but there was also no $Cl2p_{3/2}$ peak in the cases of DCMOS and CDMOS. The peak absence was due to an absence of chlorine atoms in the LB films, rather than to attenuation of the chlorine signal by the hydrocarbon layer, because the escape depth of photoelectrons of Cl2p in LB films was reported to be larger than 3 nm.[21,22] These results suggest that the chlorosilyl residues of TCOS, DCMOS, and CDMOS molecules should be eliminated by rapid hydrolysis with water just after spreading on the water surface. As the results of hydrolysis, they are transformed to hydroxyalkylsilanes.

The next problem is to decide whether the resultant hydroxysilane residues of the film molecules may condense or not, during the measurement of isotherms. Figure 8 is the pH dependence of π–A isotherms of CDMOS monolayers measured under a constant strain rate of 10% min^{-1}. With decreasing pH of the subphase, the shape of isotherms changes from the expanded to the condensed type as seen in Fig. 8. It was reported that the pK_a of the orthosilicic acid, $Si(OH)_4$ is 9.8.[12] The presence of the C_{18} chain is expected to increase the pK_a of the hydroxysilane residue. At pH 12, a significant fraction of hydroxysilane residues should be ionized considering the pK_a of 9.8. This should be the cause of the large expansion of the isotherm, due to the repulsion among the ionized hydrophilic groups of alkylhydroxysilane molecules at pH 12. In contrast, no ionization of the hydroxysilane residues should occur at pH 5.6 (distilled water) considering the pK_a, and lack of condensation reactions occurring among the hydroxysilane residues in a neutral condition within 30 min as shown by the isotherms in Fig. 9. Thus, the isotherms of CDMOS at the distilled water surface in Fig. 5 are considered to be those of dimethyl(octadecyl)-hydroxysilane monolayers.

It is well known that the condensation reaction among hydroxysilane residues is accelerated in acidic conditions. The change of shape of the isotherms in Fig. 8 by decreasing pH means that the condensation reaction proceeded effectively at lower pH within 30 min or so before measuring the isotherms. The collapse pressure increases once, with decreasing pH and then decreases at lower pH via a maximum. Data are not shown here but isotherms of CDMOS monolayers at pH 2 expanded with increasing elapsed time before compression; the limiting molecular areas at 6 and 13 h after spreading are 0.26 nm^2/molec. The collapse pressure decreases with increasing time; they are 23 mN m^{-1} at 6 h and less than 20 mN m^{-1} at 13 h, respectively. Thus, it is expected that monolayers will be rather unstable with lower collapse pressure when CDMOS molecules are transformed completely to dimers. This may be due to the lack of hydrophilicity of the resultant Si–O–Si groups as the hydrophilic moiety of the dimer molecules.

Figure 9 shows the temporal change of the shape of π–A isotherms of CDMOS monolayers caused by adding a small amount of distilled water to the spreading solution. The added water induced rapid hydrolysis of the chlorosilane residues in the solution, but dimerization of the resultant hydroxysilane residues was very slow in neutral conditions as suggested by the change of the shape of isotherms shown here. By comparing the shape of the isotherm of the sample (D) in Fig. 9 with that at pH 2 and 2.5 in Fig. 8, even an extended period of 17 d is not enough to complete dimerization of dimethyl(octadecyl)hydroxysilane in a neutral condition.

We estimated fractions of condensates among hydroxysilane residues from the atomic concentration ratios of Si to O using XPS data of LB samples on the gold substrates as follows. A large amount of water was added to the hexane solution of TCOS with vigorous agitation and the precipitated polymer was separated by filtration after standing over night. After the polymer was dried completely in a vacuum, a small amount was set on a gold-covered glass substrate and melted

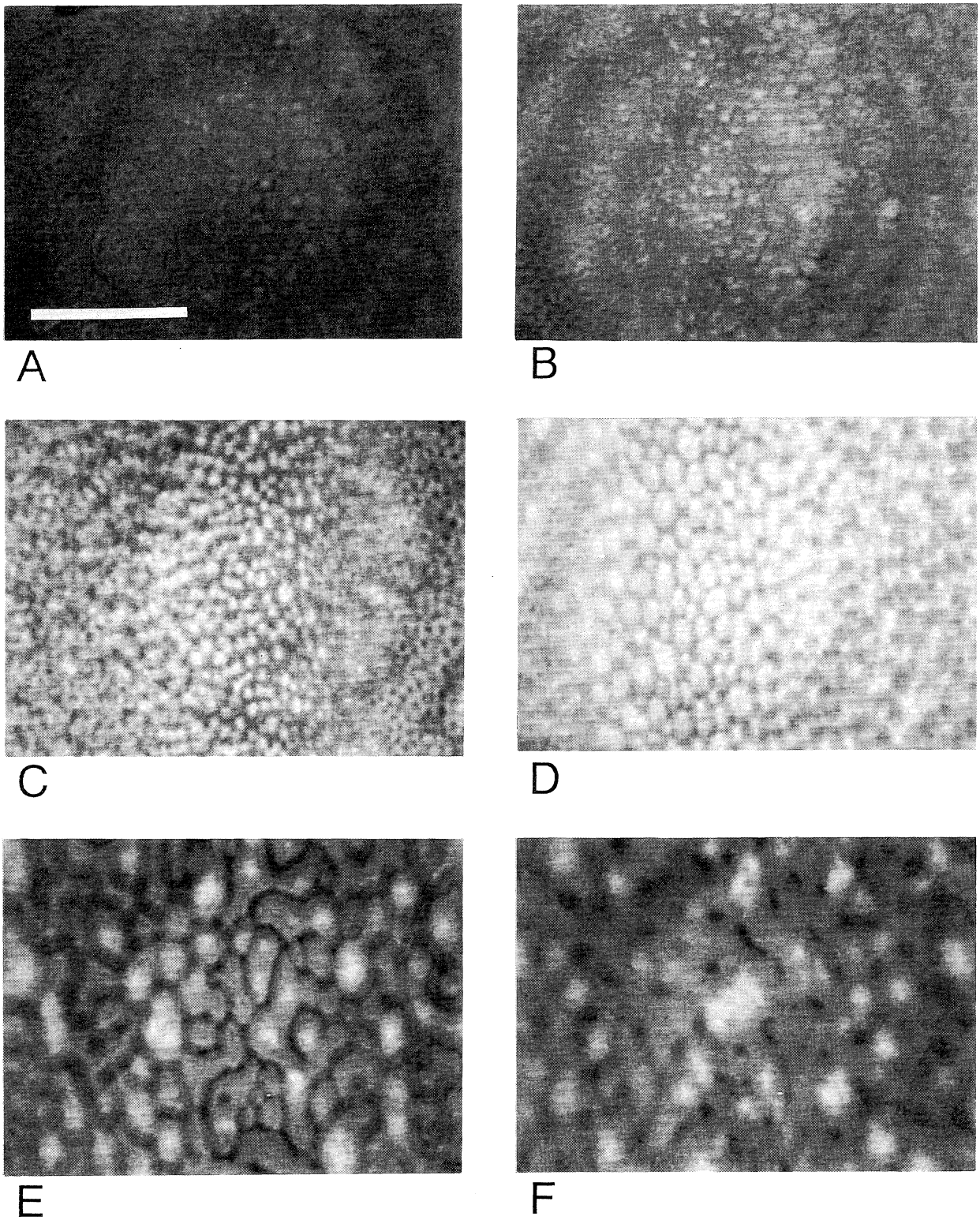

Fig. 6. BAM images of the spread monolayers of CDMOS during measurement of the isotherm in Fig. 5. The scale bar in (A) represents 300 μm. (See text for details.)

in a vacuum to adhere to the substrate. The hydroxysilane residues were expected to condense completely to form polysiloxane with this experimental procedure.

The first row of Table 1 gives the calculated atomic concentration ratio of Si to O of this polymer and that estimated from the satellite-subtracted integrated XPS peak intensities of Si2s at 153.8 eV and O1s at 532.4 eV in Fig. 7, divided by their elemental sensitivity factors. A polymer from DCMOS was obtained using the same procedure, and the atomic concentration ratios of this polymer are given in the second row

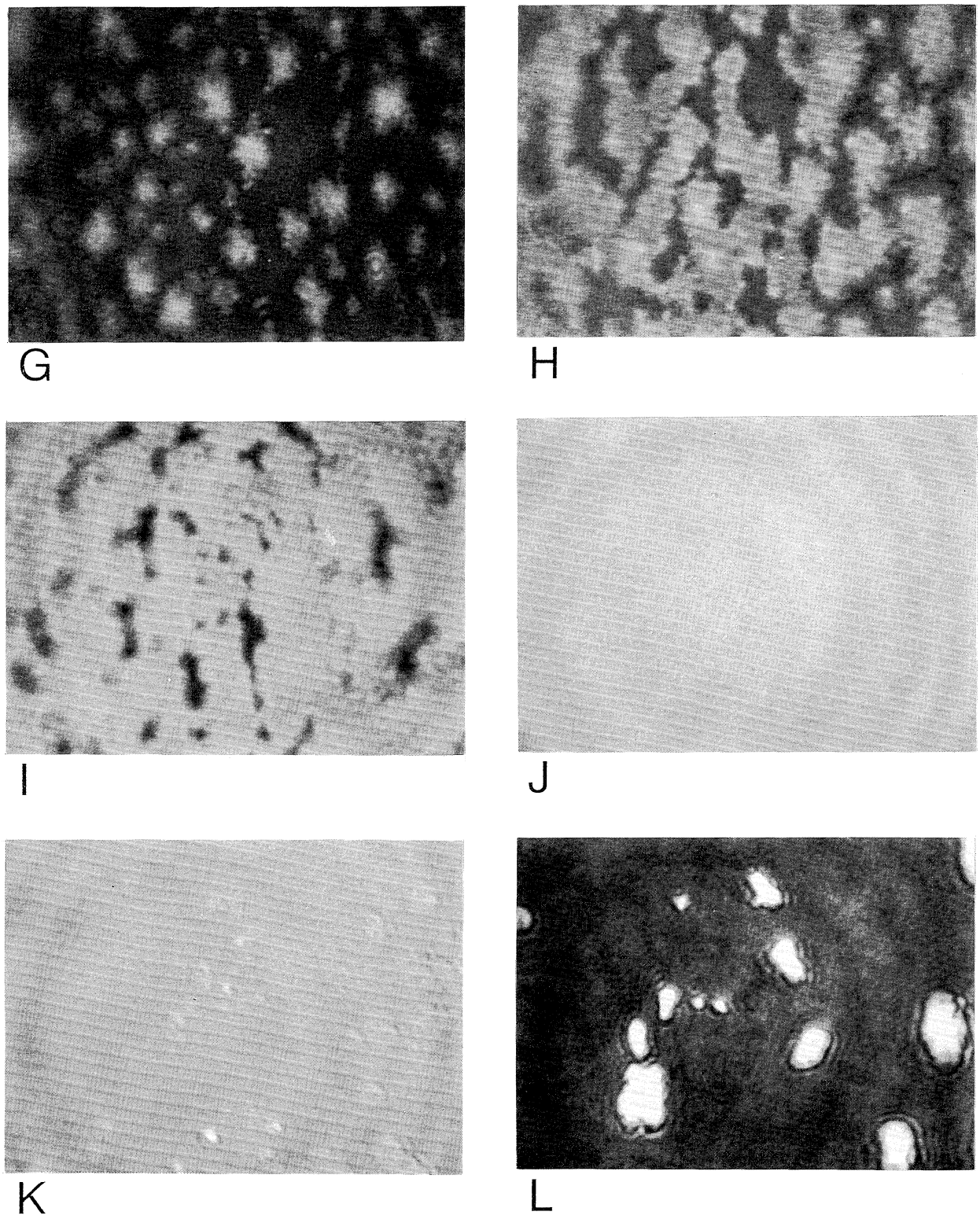

Fig. 6. (Continued).

of the table. A dimer of CDMOS was obtained by adding a large amount of distilled water to the hexane solution of it. However, as the dimer did not precipitate, the XPS sample was prepared by casting the solution on the substrate and drying it completely. The atomic concentration ratios of Si to O of the dimer from CDMOS are given in the third row of the Table 1. Those of silica (fused quartz) are given in the fourth row for comparison.

For all four polymer and dimer samples, the atomic concentration ratios of Si to O calculated for the completely condensed structures and those estimated by the XPS measurements coincided very well. These facts confirm the reli-

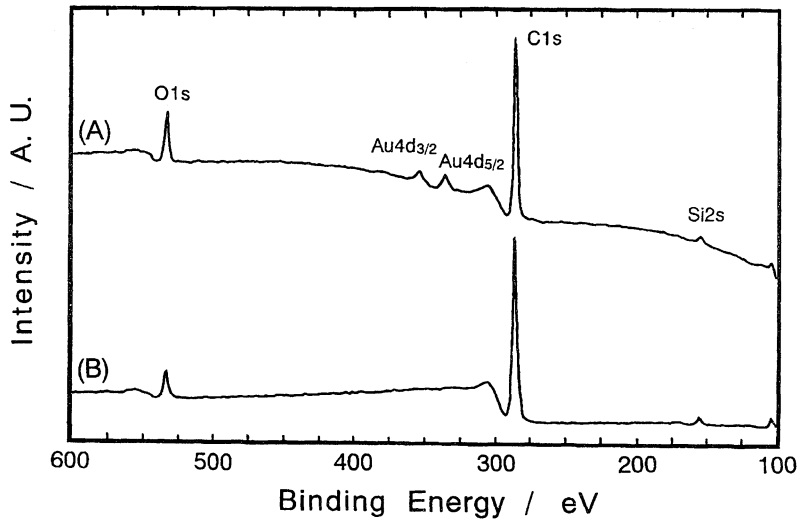

Fig. 7. XPS survey spectra of OTCS polymer and 5-layer LB films of OTCS on the gold covered glass substrates; (A) OTCS LB films, (B) OTCS polymer. (See text for details).

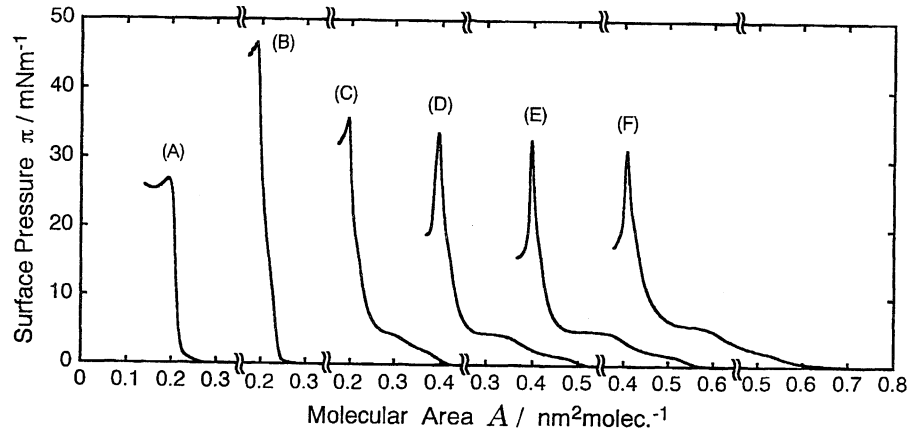

Fig. 8. pH dependence of π–A isotherms of DMOCS spread monolayers measured at time of observation of 600 s. All monolayers were allowed to stand for 30 min before compression; (A) pH = 2.0, (B) pH = 2.5, (C) pH = 3.0, (D) pH = 3.5, (E) distilled water (pH = 5.6, (F) pH = 12.0. (See text for details).

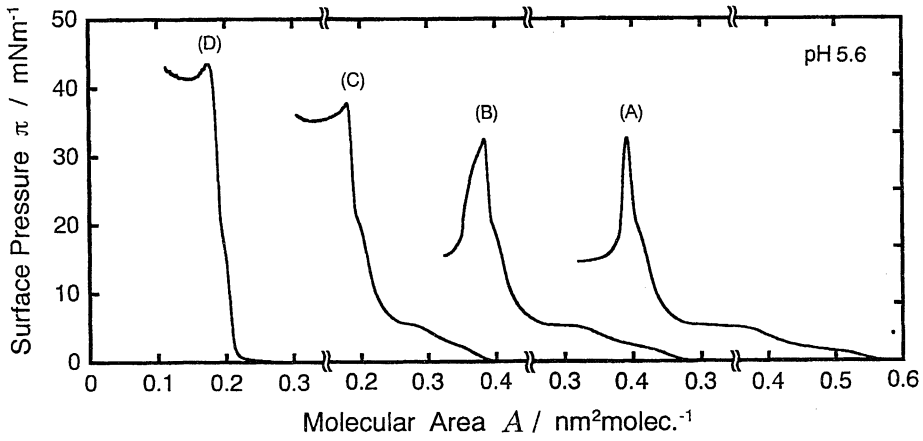

Fig. 9. Temporal change of the shape of π–A isotherms of DMOCS spread monolayers on the distilled water surface measured at time of observation of 600 s. Elapsed time after adding a small amount of water to the spreading solution are (A) 30 min, (B) 13 h, (C) 3 d, (D) 17 d.

Table 1. Atomic Concentration Ratios of Si and O Calculated for the Corresponding Molecular Structures, the Estimated Ratios of Si to O from XPS Measurements, and the Calculated Degrees of Condensation

	Binding energy/eV		Atomic concentration ratio calculated for the molecular structures		Atomic concentration ratio estimated from XPS result			Degree of condensation[e]
Surface	Si(2s)	O(1s)	%Si	%O	%Si(2s)	%O(1s)		%
OTCS polymer on Au	153.4 (±0.13)	532.2 (±0.08)	40.0	60.0	40.0	60.0	(±0.52)	100
MODCS polymer on Au	152.8 (±0.06)	531.9 (±0.05)	50.0	50.0	49.6	50.4	(±0.30)	100
DMOCS dimer on Au	152.3 (±0.02)	531.6 (±0.02)	66.6	33.3	66.2	33.8	(±0.54)	100
Fused quartz	154.3 (±0.08)	532.7 (±0.07)	33.3	66.6	33.6	66.4	(±0.75)	
OTCS LB film[a]	153.8 (±0.10)	532.4 (±0.07)	25.0	75.0[b]	26.5	73.5	(±0.41)	15.5
MODCS LB film[a]	153.2 (±0.04)	532.0 (±0.04)	33.3	66.6[c]	34.7	65.3	(±0.20)	13.7
DMOCS LB film[a]	152.6 (±0.05)	531.9 (±0.04)	50.0	50.0[d]	49.7	50.3	(±0.79)	0

a) 5-Layer LB films on the gold-covered glass substrate. b) Calculated for the trihydroxysilane structure. c) Calculated for the dihydroxysilane structure. d) Calculated for the monohydroxysilane structure. e) Calculated from the atomic concentration ratios of Si to O.

ability of the XPS method.

LB samples of TCOS, DCMOS, and CDMOS were transferred onto gold-covered glass plates at 30, 22, and 13 $mN\,m^{-1}$, respectively, for five layers by the conventional vertical dipping method. The fifth row gives the estimated atomic concentration ratio of the TCOS LB film. If TCOS molecules condense to polymer completely after hydrolysis in the monolayer, the ratio of Si to O should be 40 to 60 as expected for the TCOS polymer in the first row. The estimated ratio from the XPS measurement coincided well with the calculated value for the trihydroxysilane structure but not completely. From the ratio of Si to O we can estimate the degree of condensation among the hydroxyl groups in the monolayer, this is given in the last column of the table. Only about 16% of the total hydroxyl groups condensed. This low degree of condensation means that TCOS molecules do not form polymer molecules in the monolayer, about half of the molecules form dimers on average. Similarly, the degree of condensation among the hydroxyl groups of dihydroxy(methyl)(octadecyl)silane is about 14%, calculated from the atomic ratio of Si to O obtained by the XPS measurement as given in the last column. This leads to three tenths of dihydroxyalkysilane molecules forming dimers on average. In the case of CDMCS, the calculated degree of condensation is almost 0 and hydroxy(dimethyl)(octadecyl)silane molecules exist in the monomeric form. The reason for these differences in degrees of condensation may be the difference in concentration of the hydroxyl groups, and, the distance among the hydroxyl groups in monolayers.

π–A isotherms in Figs. 1, 3, and 5 correspond with those of trihydroxy(octadecyl)silane including dimers in some parts, dihydroxy(methyl)(octadecyl)silane including dimers in some parts, and hydroxy(dimethy)(octadecyl)silane monolayers, respectively.

Thus, condensation reaction rates among hydroxysilane residues in the monolayers should be very slow under neutral conditions at the water surface.

Conclusions

We can conclude that TCOS, DCMOS, and CDMOS molecules are rapidly hydrolyzed in the monolayer at the water surface after spreading, because there were no chlorine peaks detected in X-ray photoelectron spectra of the LB films even under higher sensitivity measurements. In acidic conditions, the condensation reactions are accelerated and the shape of the isotherms changes with time after spreading by forming polymers or the dimer. We can obtain fractions of the condensed hydroxysilane residues at any time after spreading by measuring X-ray photoelectron spectra of the LB films and by calculating atomic concentration ratios of Si to O from integrated peak intensities and the sensitivity factors of each element.

BAM observation of the monolayers during the measurements of isotherms showed that monolayers of all three compounds had no optical anisotropy. BAM images also showed that CDMOC monolayers pass a very unusual two-step phase transition in the liquid-expanded state. For the monolayers of DCMOS and CDMOS, BAM images showed that partial collapse started already in what are called solid film regions.

References

1) R. M. Leblanc and C. Salesse, "Thin Solid Films," in "Proc. 6th Intern. Confr. Organized Molecular Films," 1994, pp. 242—244.
2) J. Sagiv, *J. Am. Chem. Soc.*, **102**, 92 (1980).
3) R. Maoz and J. Sagiv, *J. Colloid Interface Sci.*, **100**, 465 (1984).
4) J. Gun, R. Iscovici and J. Sagiv, *J. Colloid Interface Sci.*, **101**, 201 (1984).
5) T. Nakagawa and K. Ogawa, *Langmuir*, **10**, 525 (1994).
6) M. E. McGovern, K. M. R. Kallury, and M. Thompson, *Langmuir*, **10**, 3607 (1994).
7) L. Netzer and J. Sagiv, *J. Am. Chem. Soc.*, **111**, 674 (1983).
8) R. Maoz, L. Netzer, J. Gun, and J. Sagiv, *J. Chim. Phys.*, **85**, 1059 (1988).
9) A. Ulman, *Adv. Mater.*, **2**, 573 (1990).
10) Y. Okahata, K. Ariga, H. Nakahara, and K. Fukuda, *J. Chem. Soc., Chem. Commun.*, **1986**, 1069.
11) K. Ariga and Y. Okahata, *J. Am. Chem. Soc.*, **111**, 5618 (1989).
12) J. Sjöblom, H. Ebeltoft, A. Bjorseth, S. E. Friberg, and C. Brancewicz, *J. Dispersion Sci. Technol.*, **15**, 21 (1994).
13) S. W. Barton, A. Goudot, and F. Rondelez, *Langmuir*, **7**,

1029 (1991).
14) L. Bourdieu, J. Daillant, D. Chatenay, A. Braslau, and D. Colson, *Phys. Rev. Lett.*, **72**, 1502 (1994).
15) T. Kato, A. Tatehana, N. Suzuki, K. Iimura, T. Araki, and K. Iriyama, *Jpn. J. Appl. Phys.*, **34**, (Part 2), L911 (1995).
16) K. Iimura, N. Suzuki, S. Sato, Y. Saito, T. Kato, and A. Tanaka, *Appl. Surface Sci.*, submitted.
17) T. Kato, *Chem. Lett.*, **1988**, 1993.
18) T. Kato, *Langmuir*, **6**, 870 (1990); T. Kato, Y. Hirobe, and M. Kato, *Langmuir*, **7**, 2208 (1991); T. Kato, A. Tatehana, and N. Suzuki, *Bull. Chem. Soc. Jpn.*, **66**, 1373 (1993).
19) H. Sapper, D. G. Cameron, and H. H. Mantsch, *Can. J. Chem.*, **59**, 2543 (1981).
20) J. Chastain, "Handbook of XPS," Perkin–Elmer Corp., (1992).
21) C. R. Brundle, H. Hopster, and J. J. Swalen, *J. Chem. Phys.*, **70**, 5190 (1979).
22) D. T. Clark, and Y. C. T. Fok, *J. Electron Spectrosc. Relat. Phenom.*, **22**, 173 (1981).